Published in final edited form as:
Neuroscience. 2008 January 24; 151(2): 476–488.

Pten deficiency in brain causes defects in synaptic structure, transmission and plasticity, and myelination abnormalities

Melissa M. Fraser, **Ildar T. Bayazitov**, **Stanislav S. Zakharenko**, and **Suzanne J. Baker***
Department of Developmental Neurobiology, St. Jude Children's Research Hospital, 332, N. Lauderdale, Memphis, TN 38105

Abstract

The phosphatidylinositol 3-kinase (PI3K) signaling pathway modulates growth, proliferation and cell survival in diverse tissue types and plays specialized roles in the nervous system including influences on neuronal polarity, dendritic branching and synaptic plasticity. The tumor-suppressor phosphatase with tensin homology (PTEN) is the central negative regulator of the PI3K pathway. Germline *PTEN* mutations result in cancer predisposition, macrocephaly and benign hamartomas in many tissues, including Lhermitte-Duclos disease, a cerebellar growth disorder. Neurological abnormalities including autism, seizures and ataxia have been observed in association with inherited *PTEN* mutation with variable penetrance. It remains unclear how loss of PTEN activity contributes to neurological dysfunction. To explore the effects of Pten deficiency on neuronal structure and function, we analyzed several ultra-structural features of Pten-deficient neurons in Pten conditional knockout mice. Using Golgi stain to visualize full neuronal morphology, we observed that increased size of nuclei and somata in Pten-deficient neurons was accompanied by enlarged caliber of neuronal projections and increased dendritic spine density. Electron microscopic evaluation revealed enlarged abnormal synaptic structures in the cerebral cortex and cerebellum. Severe myelination defects included thickening and unraveling of the myelin sheath surrounding hypertrophic axons in the corpus callosum. Defects in myelination of axons of normal caliber were observed in the cerebellum, suggesting intrinsic abnormalities in Pten-deficient oligodendrocytes. We did not observe these abnormalities in wild-type or conditional *Pten* heterozygous mice. Moreover, conditional deletion of *Pten* drastically weakened synaptic transmission and synaptic plasticity at excitatory synapses between CA3 and CA1 pyramidal neurons in the hippocampus. These data suggest that Pten is involved in mechanisms that control development of neuronal and synaptic structures and subsequently synaptic function.

Keywords

PTEN; PI3K; brain; neurons; myelin; hypertrophy; synaptic plasticity

The tumor suppressor PTEN (phosphatase and tensin homolog, deleted on chromosome 10) is important in the modulation of cell growth, proliferation and survival. Inactivating mutations in both alleles of *PTEN* occur in diverse tumor types including glioblastoma multiforme (Chow and Baker, 2006). Consistent with the two-hit hypothesis of tumor suppression, inherited mutations in *PTEN* are associated with cancer predisposition, and the second allele of *PTEN*

*To whom correspondence should be addressed: Suzanne.Baker@stjude.org; Phone: (901) 495-2254; FAX: (901) 495-2270.
Section Editor: John L.R. Rubenstein, Developmental Neuroscience

is inactivated in tumors arising in these patients. This indicates that loss of both *PTEN* alleles is important for tumorigenesis. Clinical manifestations of inherited *PTEN* mutation occur with highly variable penetrance and also include benign hamartomas in multiple tissues, macrocephaly, seizures, ataxia, mental retardation and autism in addition to cancer predisposition (Ali et al., 1999, Goffin et al., 2001, Eng, 2003, Butler et al., 2005). Changes in PTEN levels have recently been linked to Alzheimer's disease (Zori et al., 1998, Goffin et al., 2001, Butler et al., 2005, Griffin et al., 2005, Rickle et al., 2006). While the tumor suppressor activity of Pten has been extensively studied in multiple tissue types, work relating Pten loss of function to neuronal dysfunction has only recently been studied. Kwon *et al*. (Kwon et al., 2006) demonstrated a link between *Pten* loss and abnormal social interactions and responses to sensory stimuli using a mouse model in which *Pten* was deleted in select post-mitotic neurons in the cerebral cortex and the hippocampus. Abnormalities in dendrites and axonal tracts were also noted. Other work has demonstrated that decreased Pten expression can increase dendritic branching of developing hippocampal neurons *in vitro* (Jaworski et al., 2005).

Pten is the central negative regulator of the phosphatidylinositol 3′-kinase (PI3K) pathway that transduces signals for growth, proliferation and survival (Vivanco and Sawyers, 2002, Sulis and Parsons, 2003). In response to extracellular growth signals, PI3K phosphorylates the 3′ position of the signaling lipid phosphatidylinositol 4,5 bisphosphate (PIP2) to generate phosphatidylinositol 3,4,5-triphosphate (PIP3). PTEN is a phosphatase that removes the phosphate from the 3′ position of PIP3, thus halting the signal transduced by PI3K. In addition to its role as a tumor suppressor, PTEN plays critical functions in normal development and homeostasis. This is illustrated clinically by the diverse phenotypic spectrum observed in individuals with germline *PTEN* mutations, as well as experimentally in a series of mouse models in which *Pten* is deleted in the germline, or selectively deleted in specific tissues. Germline deletion of *Pten* caused embryonic lethality in mice, while *Pten* heterozygous mice survived, but developed tumors in the endometrium, liver, prostate, adrenal gland, gastrointestinal tract, thyroid and thymus (Suzuki et al., 1998, Podsypanina et al., 1999, Raftopoulou et al., 2004). Tissue-specific deletion of *Pten* results in tumors in the prostate, testis, skin, liver, and mammary glands (Di Cristofano et al., 1998, Suzuki et al., 2001, Li et al., 2002, Kimura et al., 2003, Trotman et al., 2003, Wang et al., 2003, Horie et al., 2004). While selective deletion of *Pten* in astrocytes can contribute to tumorigenesis in brain when combined with other genetic mutations (Holland et al., 2000, Xiao et al., 2002), deletion of *Pten* alone did not induce brain tumors in mice. Instead, conditional loss of *Pten* in different cell types in the nervous system resulted in alterations in cell migration, cell number and cell size (Backman et al., 2001, Groszer et al., 2001, Kwon et al., 2001, Marino et al., 2002). Indeed, the defects in cell migration and cell size regulation observed in *Pten*-deficient granule neurons of the cerebellum created a mouse model with many histopathological features of human Lhermitte-Duclos disease (Backman et al., 2001, Kwon et al., 2001). Hypertrophy of Pten-deficient neurons was dependent on activity of the rapamycin-sensitive complex of the serine-threonine kinase mTor (Kwon et al., 2003).

We and others previously reported that conditional knock-out of *Pten* in a substantial proportion of neurons and astrocytes throughout the brain caused severe progressive macrocephaly, seizures, ataxia and premature death. Abnormalities in the brain included neuronal migration defects in the hippocampus and cerebellum, increased nuclear and soma size of both neurons and astrocytes, and a low level of proliferation of astrocytes in the adult brain with no detectable tumor growth (Fraser et al., 2004, Wei et al., 2006). To gain insights into the functional and structural abnormalities associated with disrupted Pten signaling in brain *in vivo*, we evaluated a number of subcellular structural features and tested synaptic transmission and synaptic plasticity in brains from mice with conditional deletion of *Pten*.

Materials and Methods

Transgenic Mice

GFAP-cre transgenic mice, a gift from David H. Gutmann (Washington University School of Medicine), were previously described (Bajenaru et al., 2002) and were used to drive expression of *cre* recombinase specifically in the nervous system of the mouse. *GFAP-cre* mice were bred with ROSA26R Cre reporter mice (Soriano, 1999) to identify cell types in which *cre*-mediated deletion occurred *in vivo* as previously described (Fraser et al., 2004). Cre activity was visualized by immunofluorescent detection of the β-galactosidase reporter. To obtain *Pten* conditional loss in the nervous system of the mouse, $Pten^{loxp/loxp}$ mice (Suzuki et al., 2001), a gift from Tak Mak (University of Toronto), were crossed with the *GFAP-cre* mice for two generations to generate $Pten^{loxp/loxp}$*;GFAP-cre* mice, (hereafter referred to as *Pten* cKO mice) as well as littermate control mice.

Immunohistochemistry

Mice were transcardially perfused with 2% paraformaldehyde (PFA) in PBS. Tissues were post-fixed in 2% PFA for 24 hours, and then fixed in 4% PFA for a further 24 hours. Tissues were then embedded in paraffin and cut into 5-μm sections. *GFAP-cre;ROSA26R* mice were transcardially perfused with 2% PFA in PBS. These tissues were post fixed in 2% PFA for 24 hours and placed in 25% sucrose in PBS for a further 24 hours. Tissues were then embedded in TBS Tissue Freezing Medium (Triangle Biomedical Sciences) for frozen sectioning at 10-μm. The $Pten^{loxp/loxp}$ allele expresses wild-type Pten until *cre*-mediated deletion. Therefore, littermate mice with the genotypes $Pten^{+/+}$*;GFAP-cre*, $Pten^{+/+}$ or $Pten^{loxp/loxp}$ without Cre served as wild-type controls and $Pten^{+/loxp}$*;GFAP-cre* mice provided *Pten* conditional heterozygote controls. We performed immunofluorescence with primary antibodies to β-galactosidase (ICN), CC-1 (Calbiochem), and Synaptophysin (Chemicon) and fluorescein isothio-cyanate or cyanine 3-conjugated secondary antibodies (Jackson Immuno Research). We used microwave antigen retrieval for all antibodies except for Synaptophysin. We performed immunohistochemistry with primary antibody against Pten (Cell Signaling), biotin labeled secondary antibody and detection by peroxidase-conjugated avidin (Elite ABC, Vector Laboratories) treated with 3,3′-diaminobenzidine substrate, followed by counter stain with hematoxylin (Vector Laboratories). We also performed standard hematoxylin and eosin (H&E) (Richard Allen Scientific) stain on paraffin sections.

Nucleolar size and number measurements

The Bioquant system (Bioquant Image Analysis Corp.) was used to outline and calculate the area of individual nucleoli from 100 neurons in layer 5 of the cerebral cortex of 4 control and 4 *Pten* cKO mouse brain tissue sections stained with H&E. The average nucleolar area per mouse was recorded and the four averages from each mouse were averaged together to produce the average area of a nucleolus in control and *Pten* cKO mice. The number of nucleoli per cell was counted for 125 layer 5 neurons of the cerebral cortex in 4 control and 4 *Pten* cKO mice on a bright field microscope at 100X magnification.

Golgi Stain

Mice were anesthetized and cervical dislocation was performed prior to removing the brain. Brain tissue was washed in 0.1M-phosphate buffer, pH 7.4 and then processed using the FD Rapid GolgiStain Kit according to the manufacturers protocol (FD Neuro Technologies). Brain tissue was immersed in impregnation solution and kept in the dark for one week and then placed in solution C for one week to finish the impregnation process. Tissues were snap frozen and sectioned at 100–200μm for development in a combination of solution D and E for ten minutes

following a series of ethanol dehydration steps ranging from 50%, 70%, 95% and 100% and Xylenes before mounting with cover slips.

Electron Microscopy

Mice were transcardially perfused with 2% PFA in PBS. Tissue was fixed in 4% Gluteraldehyde in PBS and post-fixed in 1% osmic acid in PBS. Tissues were dehydrated in an ethanol gradient from 50% to 100% and then embedded in Spurr resin. Semi-thin sections cut at 700–900 angstroms were stained with 1% Toluidine blue (Electron Microscopy sciences) in sodium borate buffer for 1 minute at 60°C. Thin sections were stained with 2% uranyl acetate and Reynolds Lead citrate and viewed with the JOEL 1200 EX electron microscope and images were obtained on the GATAN or AMT digital camera system.

Electrophysiology

Hippocampal slices were prepared from *Pten* cKO and wild-type littermate mice. Slices were continuously superfused with artificial cerebrospinal fluid (ACSF) containing 125 mM NaCl, 2.5 mM KCl, 2 mM $CaCl_2$, 2 mM $MgSO_4$, 1.25 mM NaH_2PO_4, 26 mM $NaHCO_3$, and 10 mM glucose, with 95% O_2 and 5% CO_2 at 30–31°C (2 ml/min). Schaffer collateral synapses were stimulated with a bipolar tungsten electrode in CA1 stratum radiatum placed 200–300 μm from the recording pipette filled with ACSF, and field excitatory postsynaptic potentials (fEPSPs) were collected using a Multiclamp 700B amplifier (Molecular Devices). In long-term potentiation (LTP) experiments, Shaffer collaterals were stimulated with a pair of stimuli (50 ms interpulse interval) at 0.033 Hz before and after induction of LTP. Stimulation intensities were chosen to evoke an fEPSP with a slope of the initial phase that is 30–35% of the slope of fEPSP evoked with a maximal stimulation. LTP was induced by a 200-Hz pulse protocol consisting of 10 trains of 200 ms stimulation at 200 Hz delivered every 5 s at baseline stimulation intensity. Data were analyzed using Clampfit 9.0 software (Molecular Devices). Results were then grouped according to mouse genotypes.

Results

Ultra-structural changes in neurons of *Pten* cKO mice

The *GFAP-cre* transgenic line (Bajenaru et al., 2002) used to drive cre activity in *Pten cKO* mice for this study induced conditional deletion of *Pten* in astrocytes throughout the brain as well as widespread deletion in neuronal populations including 80–90% of hippocampal neurons and cerebellar granule neurons, and 50–80% of pyramidal neurons in the cerebral cortex (Fraser et al., 2004). Pten-deficient neurons consistently demonstrated cell autonomous increases in the size of nuclei and somata (Fraser et al., 2004). We further evaluated the ultra-structural features of neurons from cerebral cortex of *Pten* cKO mice using electron microscopy. There were several obvious changes in the Pten-null pyramidal neurons in the cerebral cortex compared with controls. Consistent with our previous studies, the increased size of nuclei and somata was readily observed in neurons from *Pten* cKO cerebral cortex compared to controls (Fig. 1A and 1B). Interestingly, *Pten* cKO mitochondria also appeared substantially enlarged.

While the somata of control neurons were easily distinguished from the more electron-dense surrounding neuropil, cytoplasm from *Pten* cKO neurons was much more electron dense, therefore it was more difficult to visualize the boundaries of somata. The increased staining of *Pten* cKO somata, viewed at higher magnification, was due to a substantial increase in the number of ribosomes (Fig. 1C and 1D). This increased ribosome density extended into the dendritic and axonal projections proximal to the somata.

Because the nucleolus is the site of ribosome biogenesis, we compared *Pten* cKO neurons to controls to determine whether the increase in ribosome number was associated with a change

in the size or number of nucleoli. We used the Bioquant system to measure the area of nucleoli contained in layer 5 pyramidal neurons from control and *Pten* cKO brains on sections stained with H&E. The average area of nucleoli in the *Pten* cKO mice ($p<0.0001$, n=400) was significantly larger than the control (n=400) (Fig. 1E). Interestingly, there did not appear to be a substantial change in the number of nucleoli per cell when comparing control to *Pten* cKO neurons ($p=0.0863$, n=500) (Fig. 1F). The dramatic increase in the size of the nucleoli is visible when comparing control and *Pten* cKO neurons in the cerebral cortex (Fig. 1G and 1H).

Pten cKO neurons contain enlarged synapses with defective synaptic structure

To study the effects of Pten-deficient hypertrophy on the complete neuronal structure including the cell body and all of its projections, we performed a Golgi stain on adult control and *Pten* cKO brains. The enlarged neuronal somata demonstrated previously by Pten immunostaining (Fraser et al., 2004) and electron microscopy (Fig. 1A and 1B), were readily visible in Golgi-stained sections of cerebral cortex from *Pten* cKO mice compared with control mice (Fig. 2A and 2B). In addition to increased soma size, the calibers of dendritic and axonal projections were also dramatically enlarged without obvious changes in branching. At higher magnification, the enlarged dendritic processes in *Pten* cKO mice showed a substantial increase in the density of spines compared to control (Fig. 2C and 2D). Further, for many spines, the morphology was abnormal and lacked the distinct mushroom-shaped termini (Fiala et al., 2002) that were characteristic for the majority of spines in neurons from control mice.

Based on the changes in dendritic spines observed by Golgi stain in *Pten* cKO mice, we used electron microscopy to evaluate synaptic structure in the cerebral cortex of adult mice in more detail. Normal synaptic connections, comprising a presynaptic terminal containing synaptic vesicles and the cognate postsynaptic terminal with postsynaptic density, were easily found in adult control cerebral cortex (Fig. 3A and C). In *Pten* cKO cortex, despite the increased density of neuronal spines, normal synaptic connections were extremely difficult to identify. Presynaptic terminals were present, although the majority were enlarged and densely packed with substantially increased numbers of synaptic vesicles. Interestingly, in greater than 60% of enlarged presynaptic terminals, the postsynaptic density was absent (Fig. 3B). Several abnormal synaptic connections were identified in which the postsynaptic density was present, but was dramatically enlarged and extended to the lateral sides of the post-synaptic terminal (Fig. 3D). A small number (<10%) of normal synapses containing both pre- and postsynaptic terminals and a normal sized postsynaptic density were detected in *Pten* cKO mice (data not shown). It is possible that these connections were made between neurons lacking Cre activity, in which Pten protein was still normally expressed. Enlarged presynaptic terminals with the increased number of synaptic vesicles also was consistent with increased immunofluorescent staining of the synaptic vesicle maker, synaptophysin in cerebral cortex of *Pten* cKO mice compared to controls (Fig. 3E and 3F).

Electron microscopy revealed that *Pten*-null cerebellar granule neurons have enlarged nuclear and soma size and contain a dense accumulation of ribosomes in the cytoplasm, similar to changes observed in neurons of the cerebral cortex (Fig. 4A and 4B). The granule neurons have distinct synaptic alterations in the molecular layer of the *Pten* cKO mice. Normal synaptic junctions containing pre- and postsynaptic terminals connected at an electron-dense postsynaptic density, were easily identified in the molecular layer of the control cerebellum (Fig. 4C and 4E). In the *Pten* cKO molecular layer based on 66 synaptic junctions, 76% of the presynaptic terminals were significantly enlarged in size and were packed with synaptic vesicles. Six percent of the synaptic junctions appeared normal (data not shown) and they were likely made by granule neurons that have retained Pten expression. The remaining 18% appeared to be partially normal with regard to the size of the presynaptic terminal or the postsynaptic density. Of the 76% of enlarged presynaptic terminals, 18% had a normal

postsynaptic density (data not shown), 30% had no visible postsynaptic density (data not shown), while 52% had a postsynaptic density that was significantly enlarged in size (Fig. 4D and 4F). More than 50% of the enlarged presynaptic terminals showed multiple synaptic junctions with multiple postsynaptic terminals (Fig. 4F). This was not observed in control cerebella.

Pten cKO neurons show defective synaptic function

Thus, *Pten* cKO neurons show numerous structural abnormalities including dramatic hypertrophy of nuclei, somata, axon and dendritic caliber, enlarged presynaptic terminals and absent or enlarged postsynaptic densities. What is the functional impact of *Pten* deletion in brain? We addressed this question by measuring synaptic transmission at excitatory synapses between CA3 and CA1 neurons (CA3-CA1 synapses) in the hippocampus. We found that synaptic transmission was drastically decreased in *Pten* cKO mice (Fig. 5A). Thus, field excitatory postsynaptic potentials (fEPSPs) were significantly impaired throughout all stimulation intensities in slices from *Pten* cKO mice compared to that in wild-type littermates ($p<0.001$. *Pten* cKO: 28 slices, 5 mice; WT mice: 27 slices, 5 mice). To determine whether this deficit in synaptic transmission is due to a deficit in presynaptic function, we measured pair-pulse ratio (PPR), which serves as a general measure of probability of neurotransmitter release. We found that at all interpulse intervals PPR was indistinguishable between *Pten* cKO and wild-type littermates (Fig. 5B. $p>0.05$, *Pten* cKO mice: 28 slices, 5 mice; WT mice: 27 slices, 5 mice). These data suggest that the dramatic deficit in synaptic transmission in *Pten* cKO mice is not due to a deficit in neurotransmitter release from presynaptic terminals but rather postsynaptic in nature. To investigate further how conditional deletion of *Pten* affects synaptic plasticity, we compared long-term potentiation (LTP) at CA3-CA1 synapses in slices from *Pten* cKO and wild-type mice. Consistent with decreased synaptic transmission in *Pten* cKO mice, LTP was drastically reduced (Fig. 5C). Thus fEPSPs measured 3 hours after induction of LTP were reduced by more than 70% in slices from *Pten* cKO mice compared to that in wild-type littermates.

Abnormal Myelination in *Pten* cKO Mice

In addition to hypertrophy of the cerebral cortex and cerebellum, the corpus callosum was also grossly enlarged. Electron microscopy revealed profound defects in myelination in the corpus callosum of *Pten* cKO mice. Sagittal section through the corpus callosum of control mice showed a cross-sectional view of axons of varying diameters tightly wrapped in myelin sheaths (Fig. 6A and 6C). In the corpus callosum from *Pten* cKO mice, many axons showed tremendous thickening of the myelin sheath, with regions of unraveling myelin (Fig. 6B and 6D). The caliber of axons was also dramatically enlarged.

The profound abnormalities seen in the myelin sheath could be a primary defect due to the loss of Pten in the oligodendrocytes or a secondary effect of neuronal hypertrophy. To determine whether *cre*-mediated recombination occurred in oligodendrocytes, we crossed the *GFAP-cre* mice with *ROSA26R* reporter mice (Soriano, 1999). The *ROSA26R* reporter contains a floxed stop signal upstream of the *lacZ* reporter gene. Upon Cre-mediated recombination, the stop signal is removed and *lacZ* is expressed from the ubiquitous *ROSA26* promoter independent of continuing expression of Cre from the *GFAP-cre* mice. Evaluation of cre activity in adult *GFAP-cre;ROSA26R* mice showed overlapping expression of CC-1, a marker for oligodendrocytes (Murtie et al., 2005, Zai and Wrathall, 2005), and the β-Gal reporter for cre activity in the corpus callosum and the white matter tracts of the cerebellum (Fig. 7A–C and 7D–F). Oligodendrocytes in *Pten cKO* mice, visualized by CC-1 immunofluorescence, showed a significant increase in nuclear (data not shown) and soma size compared with controls in both the corpus callosum and cerebellar white matter tracts (Fig. 7G–H and 7I–J).

In the cerebellum, loss of Pten occurred in the majority of the granule neurons, while Pten expression was retained in Purkinje cells (Fig. 8A and 8B), mossy and climbing fibers (data not shown). Unlike the hypertrophic axons observed in the corpus callosum, there was no substantial change in the size of the axonal diameters of the cells that extend processes into the cerebellar white matter tracts, which is consistent with Purkinje cells, mossy and climbing fibers maintaining Pten expression. However, thickened myelin sheaths as well as decreased myelin compaction were still observed in *Pten* cKO mice compared with the control (Fig. 8C and 8D), suggesting that myelination abnormalities may arise, at least in part, through intrinsic defects in Pten-deficient oligodendrocytes.

Discussion

Pten function has been studied in multiple tissue types through tissue-specific knock-out mice, showing roles for Pten in proliferation, survival and cell size regulation, depending on the context (Sulis and Parsons, 2003, Chow and Baker, 2006). As a negative regulator of PI3K signaling, Pten loss of function is often associated with constitutive activation of downstream effectors in this pathway including the serine-threonine kinases Akt and mTor. A number of *in vitro* studies have shown specific specialized functions for PI3K signaling in aspects of neuronal development including neurite growth, growth cone dynamics, axon specification and dendritic arborization (Sanchez et al., 2001, Menager et al., 2004, Jaworski et al., 2005, Jiang et al., 2005, Kumar et al., 2005, Laurino et al., 2005, Chadborn et al., 2006). While these studies demonstrate a critical role for this pathway in neuronal development, they employ exogenous growth factor stimulation with knock-down of endogenous proteins, or constitutively active or inactive mutants. *In vivo* analysis of conditional knock-out mice reveals the effects of pathway deregulation in the context of physiological growth factor signaling. Several distinct brain-specific conditional knock-out models have shown hypertrophy of nuclei and somata of Pten-deficient neurons (Backman et al., 2001, Groszer et al., 2001, Kwon et al., 2001, Marino et al., 2002, Fraser et al., 2004).

Electron microscopic detection of high ribosome density in hypertrophic Pten-deficient neurons and increased nucleolar size is consistent with our previous report that hypertrophy of Pten-deficient neurons required signaling through the rapamycin-sensitive mTor complex (Kwon et al., 2003), which functions in part to increase production of translational machinery (Ruggero and Pandolfi, 2003, Fingar and Blenis, 2004, Ruggero and Sonenberg, 2005). Numerous reports have indicated a role for mTor in synaptic plasticity mediated at least in part through regulation of localized protein translation in dendrites (Tang et al., 2002, Cammalleri et al., 2003, Si et al., 2003, Takei et al., 2004, Gong et al., 2006).

The increase in spine number and alterations in synaptic structure in *Pten* cKO brain could be a generalized hypertrophic effect on the cell, or reflect a specific role for Pten signaling in synaptic function. In Drosophila, overexpression of PI3K or AKT induced the formation and the maintenance of supernumerary synapses in developing motor neurons and mature projection neurons respectively. However, increasing neuronal size via the epidermal growth factor did not affect synapse number or morphology, suggesting that size regulation and synaptic regulation are distinct processes influenced by the PI3K pathway (Martin-Pena et al., 2006). Similar to our observations, work by Kwon et al. (Kwon et al., 2006) supports a direct role of Pten expression in maintaining normal synapse structure. In this study, loss of Pten expression in a subset of differentiated neurons in the cerebral cortex and dentate gyrus resulted in hypertrophic axons and dendrites and significant enlargement of presynaptic terminals, which contained multiple synaptic densities and large numbers of synaptic vesicles. Evaluation of PI3K signaling in cultured hippocampal neurons also showed that combined activation of Ras and PI3K induced increased dendritic complexity while constitutively activated forms of PI3K or Akt caused increased dendritic size and disrupted dendritic shape in the absence of

altered Ras signaling (Kumar et al., 2005). The tuberous sclerosis complex normally functions to inhibit mTor activity, and this inhibition can be relieved by PI3K activation through activated Akt. Loss of *Tsc1* or *Tsc2* caused increased soma size and elongated dendritic spines with enlarged bulbous heads in hippocampal pyramidal neurons (Tavazoie et al., 2005), reminiscent of the alterations observed in *Pten* cKO mice.

What is the functional consequence of the hypertrophic and abnormal synaptic structures resulting from mutation of different PI3K pathway effectors? Electrophysiological recordings from *Pten* cKO hippocampus indicated strong deficits in synaptic transmission, most likely due to compromised postsynaptic function. This is consistent with the structural abnormalities in postsynaptic densities revealed by electron microscopy. No general defects in presynaptic neurotransmitter release as measured by PPR were observed in *Pten* cKO hippocampus. Analysis of hippocampal slice cultures with conditional deletion of *Tsc1* similarly showed normal presynaptic function, with no detectable abnormalities in PPR or frequency of spontaneous miniature EPSCs (mEPSCs), but abnormal postsynaptic function, shown by increased spontaneous mEPSC amplitude and an altered ratio of currents mediated by AMPA receptors and NMDA receptors (Tavazoie et al., 2005). Overexpression of PI3K in Drosophila abdominal larval motor neurons also showed a functional consequence with enhanced spontaneous and evoked neurotransmitter release (Martin-Pena et al., 2006). *Pten* cKO mice showed a number of profound structural defects in multiple cell types, therefore the functional abnormalities that we observed in synaptic transmission and plasticity may not be exclusively associated with cell-autonomous defects in the function of Pten-deficient neurons. Recent studies showed that conditional deletion of *Tsc1*, which was achieved using the same *GFAP-cre* transgenic mouse used in our study, caused impaired LTP and was associated with learning deficits. While these deficiencies in hippocampal function may have been the result of abnormal glutamate homeostasis in *Tsc1* cKO mice, it is possible that multiple cell types lacking *Tsc1* contributed to the phenotype (Zeng et al., 2007). Future studies directing Pten loss exclusively in neurons will allow the elucidation of which abnormalities are cell-autonomous. However, we clearly demonstrated that *Pten* deletion in brain has profound functional and structural consequences.

We also observed dramatic changes in myelination in both the corpus callosum and white matter tracts of the cerebellum in *Pten cKO* mice compared to controls. Enlarged oligodendrocyte somata were accompanied by increased thickness of the myelin sheath and myelin decompaction. Several lines of evidence indicate a role for PI3K signaling in myelination. IGF-1, which activates PI3K signaling, promotes the expression of myelin-associated protein markers in cultured Schwann cells. Further, introduction of a constitutively active Akt into transplanted nerve segments showed increased myelination in an *in vivo* transplant model (Ogata et al., 2004). Mice lacking the gene encoding the endopeptidase Bace-1 showed delayed myelination and decreased myelin thickness associated with a decrease in cleaved neuregulin and a resulting decrease in phosphorylated Akt (Hu et al., 2006).

The abnormal myelination by Pten-deficient oligodendrocytes ensheathing axons from neurons that still express Pten in the cerebellum strongly suggests that Pten loss caused cell-autonomous defects in oligodendrocytes. However, multiple factors could contribute to the profound oligodendrocyte hypertrophy and defects in myelination observed in the corpus callosum of *Pten* cKO mice where *Pten* was deleted in multiple cell types. The loss of Pten in neurons significantly increased the full neuronal structure, which could lead to increased myelin, as size and length of the dendrites and axon is known to influence myelination (Michailov et al., 2004). Also, the progressive increase in caliber of Pten-null axons could create increased pressure on the myelin sheath, potentially resulting in decompaction. Additionally, it has been demonstrated that astrocytes have the capacity to promote myelination by reacting to the action potential firing of neighboring neurons. The action potential from a neuron triggers the

astrocytes to release leukemia inhibitory factor (LIF), which stimulates myelination by the oligodendrocytes (Ishibashi et al., 2006). Perhaps hypertrophic astrocytes observed in *Pten* cKO brain (Fraser et al., 2004) are capable of producing more LIF, leading to increased myelination.

Myelin defects in the cerebellar white matter tracts strongly suggest intrinsic defects in Pten-deficient oligodendrocytes. In this region, cre activity is observed in oligodendrocytes which are hypertrophic in *Pten* cKO mice and associated with increased myelin thickness and decompaction. However, the axons of the Purkinje cells, mossy fibers and climbing fibers, found in the white matter tracts, are similar in size compared with the controls due to the absence of cre activity and the retention of Pten expression in these cell types. This indicates the potential for a cell autonomous defect in myelination with the loss of Pten in oligodendrocytes. Selective deletion of Pten in oligodendrocytes would be ideal to further determine the precise role that Pten plays in myelination.

The changes in cellular ultra-structure of *Pten* cKO mice illustrate the spectrum of abnormalities that could occur in the absence of functional PTEN in the brain. Observations of ultrastructural defects in cerebella of *Pten* cKO mice are consistent with changes observed in human Lhermitte-Duclos disease (LDD), which occurs in patients with inherited *PTEN* mutation. In the hypertrophic lesions in LDD, the wild-type *PTEN* allele is inactivated resulting in the complete loss of functional PTEN (Eng and Peacocke, 1998). Electron microscopy and Golgi stain analyses demonstrated hypertrophic granule neurons accompanied by increases in ribosomes, similar to our results. The dendritic spines were thickened and pre-synaptic terminals were enlarged and contained dense regions of synaptic vesicles (Gessaga, 1980, Reznik and Schoenen, 1983, Marano et al., 1988, Ferrer et al., 1990, Hair et al., 1992). Other defects observed in *Pten* cKO brains reflect the spectrum of abnormalities that may result from complete Pten inactivation in different cell populations. Neurological defects in patients with inherited *PTEN* germline mutations may be due in part to second hits in the remaining wild-type allele in subpopulations of cells. The severity of disease would be associated with the number and types of cells that acquire the second mutation in the normal *PTEN* allele and the developmental stage at which such a somatic mutation is acquired. The stochastic nature of this event likely contributes to the highly variable neurological phenotype associated with inherited germline *PTEN* mutations.

Acknowledgements

We thank Dr. Jim Morgan for helpful discussions and Dr. Richard Smeyne for help with the BioQuant system. We thank Jennifer Parris for sectioning Golgi stained tissue. We thank Linda Mann and Sharon Frase of the St Jude Children's Research Hospital and University of Memphis, respectively for their expertise in electron microscopy. This work was supported by NIH grants NS044172 and CA096832 from the National Institutes of Health (SJB), Searle Scholars Programs and Whitehall Foundation (SSZ) and by the American Lebanese and Syrian Associated Charities.

List of Abbreviations

Pten
: phosphatase and tensin homolog, deleted on chromosome 10

PI3K
: phosphatidylinositol 3-kinase

PIP2
: phosphatidylinositol 4,5 bisphosphate

PIP3
: phosphatidylinositol 3,4,5-triphosphate

GFAP
glial fibrillary acidic protein

β-gal
β-galactosidase

fEPSPs
field excitatory postsynaptic potentials

mEPSCs
miniature excitatory postsynaptic currents

PPR
pair-pulse ratio

LTP
long-term potentiation

LDD
Lhermitte-Duclos disease

References

Ali IU, Schriml LM, Dean M. Mutational spectra of PTEN/MMAC1 gene: a tumor suppressor with lipid phosphatase activity. J Natl Cancer Inst 1999;91:1922–1932. [PubMed: 10564676]

Backman SA, Stambolic V, Suzuki A, Haight J, Elia A, Pretorius J, Tsao MS, Shannon P, Bolon B, Ivy GO, Mak TW. Deletion of Pten in mouse brain causes seizures, ataxia and defects in soma size resembling Lhermitte-Duclos disease. Nat Genet 2001;29:396–403. [PubMed: 11726926]

Bajenaru ML, Zhu Y, Hedrick NM, Donahoe J, Parada LF, Gutmann DH. Astrocyte-specific inactivation of the neurofibromatosis 1 gene (NF1) is insufficient for astrocytoma formation. Mol Cell Biol 2002;22:5100–5113. [PubMed: 12077339]

Butler MG, Dasouki MJ, Zhou XP, Talebizadeh Z, Brown M, Takahashi TN, Miles JH, Wang CH, Stratton R, Pilarski R, Eng C. Subset of individuals with autism spectrum disorders and extreme macrocephaly associated with germline PTEN tumour suppressor gene mutations. J Med Genet 2005;42:318–321. [PubMed: 15805158]

Cammalleri M, Lutjens R, Berton F, King AR, Simpson C, Francesconi W, Sanna PP. Time-restricted role for dendritic activation of the mTOR-p70S6K pathway in the induction of late-phase long-term potentiation in the CA1. Proc Natl Acad Sci U S A 2003;100:14368–14373. [PubMed: 14623952]

Chadborn NH, Ahmed AI, Holt MR, Prinjha R, Dunn GA, Jones GE, Eickholt BJ. PTEN couples Sema3A signalling to growth cone collapse. J Cell Sci 2006;119:951–957. [PubMed: 16495486]

Chow LM, Baker SJ. PTEN function in normal and neoplastic growth. Cancer Lett. 2006

Di Cristofano A, Pesce B, Cordon-Cardo C, Pandolfi PP. Pten is essential for embryonic development and tumour suppression. Nat Genet 1998;19:348–355. [PubMed: 9697695]

Eng C. PTEN: one gene, many syndromes. Hum Mutat 2003;22:183–198. [PubMed: 12938083]

Eng C, Peacocke M. PTEN and inherited hamartoma-cancer syndromes. Nat Genet 1998;19:223. [PubMed: 9662392]

Ferrer I, Marti E, Guionnet N, Bella R, Serrano T, Towse J, Conesa G, Isamat F. Studies with the Golgi method in central gangliogliomas and dysplastic gangliocytoma of the cerebellum (Lhermitte-Duclos disease). Histol Histopathol 1990;5:329–336. [PubMed: 1724930]

Fiala JC, Spacek J, Harris KM. Dendritic spine pathology: cause or consequence of neurological disorders? Brain Res Brain Res Rev 2002;39:29–54. [PubMed: 12086707]

Fingar DC, Blenis J. Target of rapamycin (TOR): an integrator of nutrient and growth factor signals and coordinator of cell growth and cell cycle progression. Oncogene 2004;23:3151–3171. [PubMed: 15094765]

Fraser MM, Zhu X, Kwon CH, Uhlmann EJ, Gutmann DH, Baker SJ. Pten loss causes hypertrophy and increased proliferation of astrocytes in vivo. Cancer Res 2004;64:7773–7779. [PubMed: 15520182]

Gessaga EC. Lhermitte-Duclos disease (diffuse hypertrophy of the cerebellum). Report of two cases. Neurosurg Rev 1980;3:151–158. [PubMed: 7231686]

Goffin A, Hoefsloot LH, Bosgoed E, Swillen A, Fryns JP. PTEN mutation in a family with Cowden syndrome and autism. Am J Med Genet 2001;105:521–524. [PubMed: 11496368]

Gong R, Park CS, Abbassi NR, Tang SJ. Roles of glutamate receptors and the mammalian target of rapamycin (mTOR) signaling pathway in activity-dependent dendritic protein synthesis in hippocampal neurons. J Biol Chem 2006;281:18802–18815. [PubMed: 16651266]

Griffin RJ, Moloney A, Kelliher M, Johnston JA, Ravid R, Dockery P, O'Connor R, O'Neill C. Activation of Akt/PKB, increased phosphorylation of Akt substrates and loss and altered distribution of Akt and PTEN are features of Alzheimer's disease pathology. J Neurochem 2005;93:105–117. [PubMed: 15773910]

Groszer M, Erickson R, Scripture-Adams DD, Lesche R, Trumpp A, Zack JA, Kornblum HI, Liu X, Wu H. Negative regulation of neural stem/progenitor cell proliferation by the Pten tumor suppressor gene in vivo. Science 2001;294:2186–2189. [PubMed: 11691952]

Hair LS, Symmans F, Powers JM, Carmel P. Immunohistochemistry and proliferative activity in Lhermitte-Duclos disease. Acta Neuropathol (Berl) 1992;84:570–573. [PubMed: 1462769]

Holland EC, Li Y, Celestino J, Dai C, Schaefer L, Sawaya RA, Fuller GN. Astrocytes give rise to oligodendrogliomas and astrocytomas after gene transfer of polyoma virus middle T antigen in vivo. Am J Pathol 2000;157:1031–1037. [PubMed: 10980141]

Horie Y, Suzuki A, Kataoka E, Sasaki T, Hamada K, Sasaki J, Mizuno K, Hasegawa G, Kishimoto H, Iizuka M, Naito M, Enomoto K, Watanabe S, Mak TW, Nakano T. Hepatocyte-specific Pten deficiency results in steatohepatitis and hepatocellular carcinomas. J Clin Invest 2004;113:1774–1783. [PubMed: 15199412]

Hu X, Hicks CW, He W, Wong P, Macklin WB, Trapp BD, Yan R. Bace1 modulates myelination in the central and peripheral nervous system. Nat Neurosci 2006;9:1520–1525. [PubMed: 17099708]

Ishibashi T, Dakin KA, Stevens B, Lee PR, Kozlov SV, Stewart CL, Fields RD. Astrocytes promote myelination in response to electrical impulses. Neuron 2006;49:823–832. [PubMed: 16543131]

Jaworski J, Spangler S, Seeburg DP, Hoogenraad CC, Sheng M. Control of dendritic arborization by the phosphoinositide-3′-kinase-Akt-mammalian target of rapamycin pathway. J Neurosci 2005;25:11300–11312. [PubMed: 16339025]

Jiang H, Guo W, Liang X, Rao Y. Both the establishment and the maintenance of neuronal polarity require active mechanisms: critical roles of GSK-3beta and its upstream regulators. Cell 2005;120:123–135. [PubMed: 15652487]

Kimura T, Suzuki A, Fujita Y, Yomogida K, Lomeli H, Asada N, Ikeuchi M, Nagy A, Mak TW, Nakano T. Conditional loss of PTEN leads to testicular teratoma and enhances embryonic germ cell production. Development 2003;130:1691–1700. [PubMed: 12620992]

Kumar V, Zhang MX, Swank MW, Kunz J, Wu GY. Regulation of dendritic morphogenesis by Ras-PI3K-Akt-mTOR and Ras-MAPK signaling pathways. J Neurosci 2005;25:11288–11299. [PubMed: 16339024]

Kwon CH, Luikart BW, Powell CM, Zhou J, Matheny SA, Zhang W, Li Y, Baker SJ, Parada LF. Pten regulates neuronal arborization and social interaction in mice. Neuron 2006;50:377–388. [PubMed: 16675393]

Kwon CH, Zhu X, Zhang J, Baker SJ. mTor is required for hypertrophy of Pten-deficient neuronal soma in vivo. Proc Natl Acad Sci U S A 2003;100:12923–12928. [PubMed: 14534328]

Kwon CH, Zhu X, Zhang J, Knoop LL, Tharp R, Smeyne RJ, Eberhart CG, Burger PC, Baker SJ. Pten regulates neuronal soma size: a mouse model of Lhermitte-Duclos disease. Nat Genet 2001;29:404–411. [PubMed: 11726927]

Laurino L, Wang XX, de la Houssaye BA, Sosa L, Dupraz S, Caceres A, Pfenninger KH, Quiroga S. PI3K activation by IGF-1 is essential for the regulation of membrane expansion at the nerve growth cone. J Cell Sci 2005;118:3653–3662. [PubMed: 16046480]

Li G, Robinson GW, Lesche R, Martinez-Diaz H, Jiang Z, Rozengurt N, Wagner KU, Wu DC, Lane TF, Liu X, Hennighausen L, Wu H. Conditional loss of PTEN leads to precocious development and neoplasia in the mammary gland. Development 2002;129:4159–4170. [PubMed: 12163417]

Marano SR, Johnson PC, Spetzler RF. Recurrent Lhermitte-Duclos disease in a child. Case report. J Neurosurg 1988;69:599–603. [PubMed: 3418394]

Marino S, Krimpenfort P, Leung C, van der Korput HA, Trapman J, Camenisch I, Berns A, Brandner S. PTEN is essential for cell migration but not for fate determination and tumourigenesis in the cerebellum. Development 2002;129:3513–3522. [PubMed: 12091320]

Martin-Pena A, Acebes A, Rodriguez JR, Sorribes A, de Polavieja GG, Fernandez-Funez P, Ferrus A. Age-independent synaptogenesis by phosphoinositide 3 kinase. J Neurosci 2006;26:10199–10208. [PubMed: 17021175]

Menager C, Arimura N, Fukata Y, Kaibuchi K. PIP3 is involved in neuronal polarization and axon formation. J Neurochem 2004;89:109–118. [PubMed: 15030394]

Michailov GV, Sereda MW, Brinkmann BG, Fischer TM, Haug B, Birchmeier C, Role L, Lai C, Schwab MH, Nave KA. Axonal neuregulin-1 regulates myelin sheath thickness. Science 2004;304:700–703. [PubMed: 15044753]

Murtie JC, Zhou YX, Le TQ, Armstrong RC. In vivo analysis of oligodendrocyte lineage development in postnatal FGF2 null mice. Glia 2005;49:542–554. [PubMed: 15578654]

Ogata T, Iijima S, Hoshikawa S, Miura T, Yamamoto S, Oda H, Nakamura K, Tanaka S. Opposing extracellular signal-regulated kinase and Akt pathways control Schwann cell myelination. J Neurosci 2004;24:6724–6732. [PubMed: 15282275]

Podsypanina K, Ellenson LH, Nemes A, Gu J, Tamura M, Yamada KM, Cordon-Cardo C, Catoretti G, Fisher PE, Parsons R. Mutation of Pten/Mmac1 in mice causes neoplasia in multiple organ systems. Proc Natl Acad Sci U S A 1999;96:1563–1568. [PubMed: 9990064]

Raftopoulou M, Etienne-Manneville S, Self A, Nicholls S, Hall A. Regulation of cell migration by the C2 domain of the tumor suppressor PTEN. Science 2004;303:1179–1181. [PubMed: 14976311]

Reznik M, Schoenen J. Lhermitte-Duclos disease. Acta Neuropathol (Berl) 1983;59:88–94. [PubMed: 6837278]

Rickle A, Bogdanovic N, Volkmann I, Zhou X, Pei JJ, Winblad B, Cowburn RF. PTEN levels in Alzheimer's disease medial temporal cortex. Neurochem Int 2006;48:114–123. [PubMed: 16239049]

Ruggero D, Pandolfi PP. Does the ribosome translate cancer? Nat Rev Cancer 2003;3:179–192. [PubMed: 12612653]

Ruggero D, Sonenberg N. The Akt of translational control. Oncogene 2005;24:7426–7434. [PubMed: 16288289]

Sanchez S, Sayas CL, Lim F, Diaz-Nido J, Avila J, Wandosell F. The inhibition of phosphatidylinositol-3-kinase induces neurite retraction and activates GSK3. J Neurochem 2001;78:468–481. [PubMed: 11483649]

Si K, Giustetto M, Etkin A, Hsu R, Janisiewicz AM, Miniaci MC, Kim JH, Zhu H, Kandel ER. A neuronal isoform of CPEB regulates local protein synthesis and stabilizes synapse-specific long-term facilitation in aplysia. Cell 2003;115:893–904. [PubMed: 14697206]

Soriano P. Generalized lacZ expression with the ROSA26 Cre reporter strain. Nat Genet 1999;21:70–71. [PubMed: 9916792]

Sulis ML, Parsons R. PTEN: from pathology to biology. Trends Cell Biol 2003;13:478–483. [PubMed: 12946627]

Suzuki A, de la Pompa JL, Stambolic V, Elia AJ, Sasaki T, del Barco Barrantes I, Ho A, Wakeham A, Itie A, Khoo W, Fukumoto M, Mak TW. High cancer susceptibility and embryonic lethality associated with mutation of the PTEN tumor suppressor gene in mice. Curr Biol 1998;8:1169–1178. [PubMed: 9799734]

Suzuki A, Yamaguchi MT, Ohteki T, Sasaki T, Kaisho T, Kimura Y, Yoshida R, Wakeham A, Higuchi T, Fukumoto M, Tsubata T, Ohashi PS, Koyasu S, Penninger JM, Nakano T, Mak TW. T cell-specific loss of Pten leads to defects in central and peripheral tolerance. Immunity 2001;14:523–534. [PubMed: 11371355]

Takei N, Inamura N, Kawamura M, Namba H, Hara K, Yonezawa K, Nawa H. Brain-derived neurotrophic factor induces mammalian target of rapamycin-dependent local activation of translation machinery and protein synthesis in neuronal dendrites. J Neurosci 2004;24:9760–9769. [PubMed: 15525761]

Tang SJ, Reis G, Kang H, Gingras AC, Sonenberg N, Schuman EM. A rapamycin-sensitive signaling pathway contributes to long-term synaptic plasticity in the hippocampus. Proc Natl Acad Sci U S A 2002;99:467–472. [PubMed: 11756682]

Tavazoie SF, Alvarez VA, Ridenour DA, Kwiatkowski DJ, Sabatini BL. Regulation of neuronal morphology and function by the tumor suppressors Tsc1 and Tsc2. Nat Neurosci 2005;8:1727–1734. [PubMed: 16286931]

Trotman LC, Niki M, Dotan ZA, Koutcher JA, Di Cristofano A, Xiao A, Khoo AS, Roy-Burman P, Greenberg NM, Van Dyke T, Cordon-Cardo C, Pandolfi PP. Pten dose dictates cancer progression in the prostate. PLoS Biol 2003;1:E59. [PubMed: 14691534]

Vivanco I, Sawyers CL. The phosphatidylinositol 3-Kinase AKT pathway in human cancer. Nat Rev Cancer 2002;2:489–501. [PubMed: 12094235]

Wang S, Gao J, Lei Q, Rozengurt N, Pritchard C, Jiao J, Thomas GV, Li G, Roy-Burman P, Nelson PS, Liu X, Wu H. Prostate-specific deletion of the murine Pten tumor suppressor gene leads to metastatic prostate cancer. Cancer Cell 2003;4:209–221. [PubMed: 14522255]

Wei Q, Clarke L, Scheidenhelm DK, Qian B, Tong A, Sabha N, Karim Z, Bock NA, Reti R, Swoboda R, Purev E, Lavoie JF, Bajenaru ML, Shannon P, Herlyn D, Kaplan D, Henkelman RM, Gutmann DH, Guha A. High-grade glioma formation results from postnatal pten loss or mutant epidermal growth factor receptor expression in a transgenic mouse glioma model. Cancer Res 2006;66:7429–7437. [PubMed: 16885338]

Xiao A, Wu H, Pandolfi PP, Louis DN, Van Dyke T. Astrocyte inactivation of the pRb pathway predisposes mice to malignant astrocytoma development that is accelerated by PTEN mutation. Cancer Cell 2002;1:157–168. [PubMed: 12086874]

Zai LJ, Wrathall JR. Cell proliferation and replacement following contusive spinal cord injury. Glia 2005;50:247–257. [PubMed: 15739189]

Zeng LH, Ouyang Y, Gazit V, Cirrito JR, Jansen LA, Ess KC, Yamada KA, Wozniak DF, Holtzman DM, Gutmann DH, Wong M. Abnormal glutamate homeostasis and impaired synaptic plasticity and learning in a mouse model of tuberous sclerosis complex. Neurobiol Dis. 2007

Zori RT, Marsh DJ, Graham GE, Marliss EB, Eng C. Germline PTEN mutation in a family with Cowden syndrome and Bannayan-Riley-Ruvalcaba syndrome. Am J Med Genet 1998;80:399–402. [PubMed: 9856571]

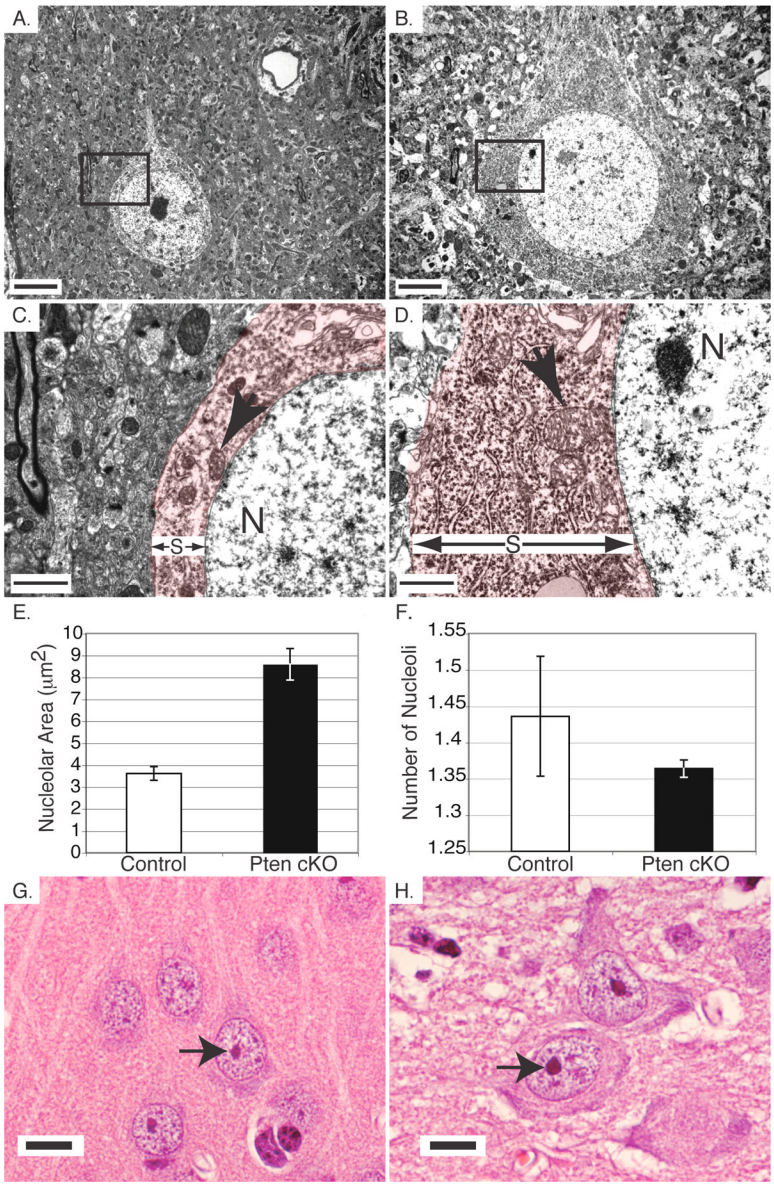

Fig. 1.

Hypertrophy of *Pten* cKO neurons was associated with increased ribosome density and increased nucleolar size. A,B. Electron microscopy of neurons in layer 5 of the cerebral cortex of control (A) and *Pten* cKO (B) mice. The boundary of the cell membrane with extra cellular matrix is less defined in the *Pten* cKO tissue compared with the control. C,D. Electron microscopy of the boxed areas from Figure 1A and 1B of control (C) and *Pten* cKO mice (D). The nucleus and mitochondria are labeled with an N and arrow, respectively. There is a dramatic increase in ribosome density and mitochondrial size in the *Pten* cKO (D) mice compared with the control (C). The increased soma size is indicated with red color and an S in between two arrows. E. The area of nucleoli in cerebral cortex neurons in control (white bar) and *Pten* cKO mice (black bar) was measured. Nucleoli were enlarged in the *Pten* cKO mice compared with the controls. F. The number of nucleoli per cell in control (white bar) and *Pten* cKO (black bar) mice were counted. There was no significant difference in the number of nucleoli per cell between control and *Pten* cKO mice. G,H. H&E stained sections of cerebral cortex pyramidal neurons from control (G) and *Pten* cKO mice (H). The increased nucleolar

size is apparent in the *Pten* cKO mice. Scale bar for A,B=5 μm, C,D=1μm and G,H=10μm. Mice were >10 weeks old. Paired t-test P values for E=0.0108 and F=0.4773.

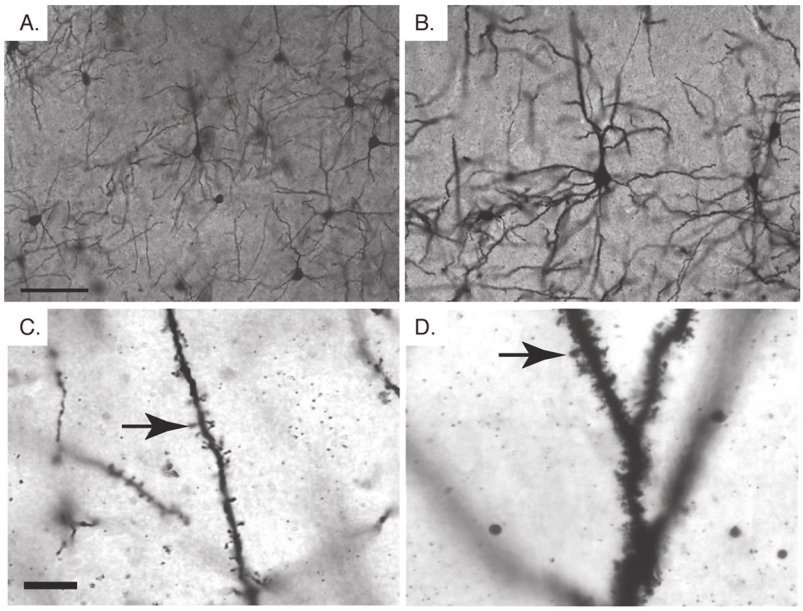

Fig. 2.

Neuronal hypertrophy in *Pten* cKO mice. A,B. Golgi stained neurons in the cerebral cortex of adult control (A) and *Pten* cKO (B) mice. Hypertrophy of *Pten* cKO neurons (B) involved the somata and all projections as compared to control neurons (A). C,D. At higher magnification, dendritic branches from control (C) and *Pten* cKO (D) mice are shown. The dendritic spines (arrow) in the control animal are spaced out along the dendrite and contain the rounded termini characteristic of mature spines. The spines (arrow) in the *Pten* cKO mice are densely packed and many lack the terminal rounded structure observed in the control spines. Mice were >10 weeks old. Scale bar for A,B=50μm and for C,D=10μm.

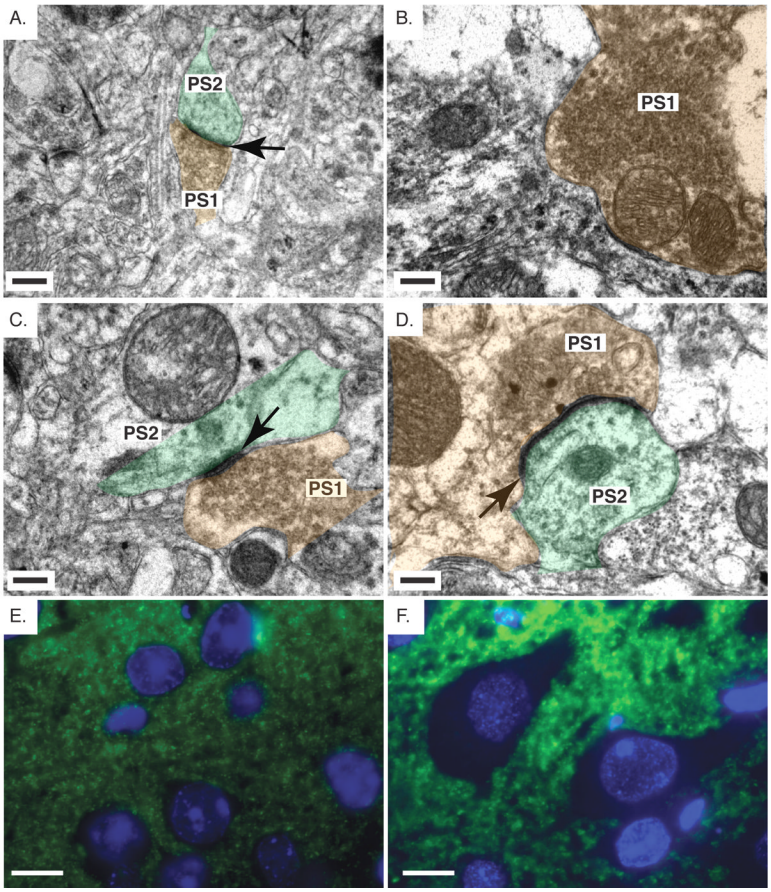

Fig. 3.

Abnormal synaptic connections in *Pten* cKO mice. A,B,C,D. Electron micrographs of the cerebral cortex from control (A,C) and *Pten* cKO mice (B,D). In the control mice, the pre- (PS1) and post- (PS2) synaptic terminals are visible. They are labeled with brown and green color, respectively. The pre-synaptic terminal is identified by the presence of synaptic vesicles. The postsynaptic density (black arrow) is also clearly visible in the control cortex. In the *Pten* cKO mice (B), the majority of the structures observed were enlarged pre-synaptic terminals, which contained a large number of synaptic vesicles (PS1) with no visible postsynaptic density. A second type of synapse was observed which had a postsynaptic density (black arrow) that extended past the region of the pre-synaptic terminal (D). E,F. Immunofluorescent staining with synaptophysin in the cerebral cortex of control (E) and *Pten* cKO mice (F) shows increased synaptophysin expression in the *Pten* cKO mice. Mice were >10 weeks old. Scale bar for A,B,C,D=0.3μm and E,F=10μm.

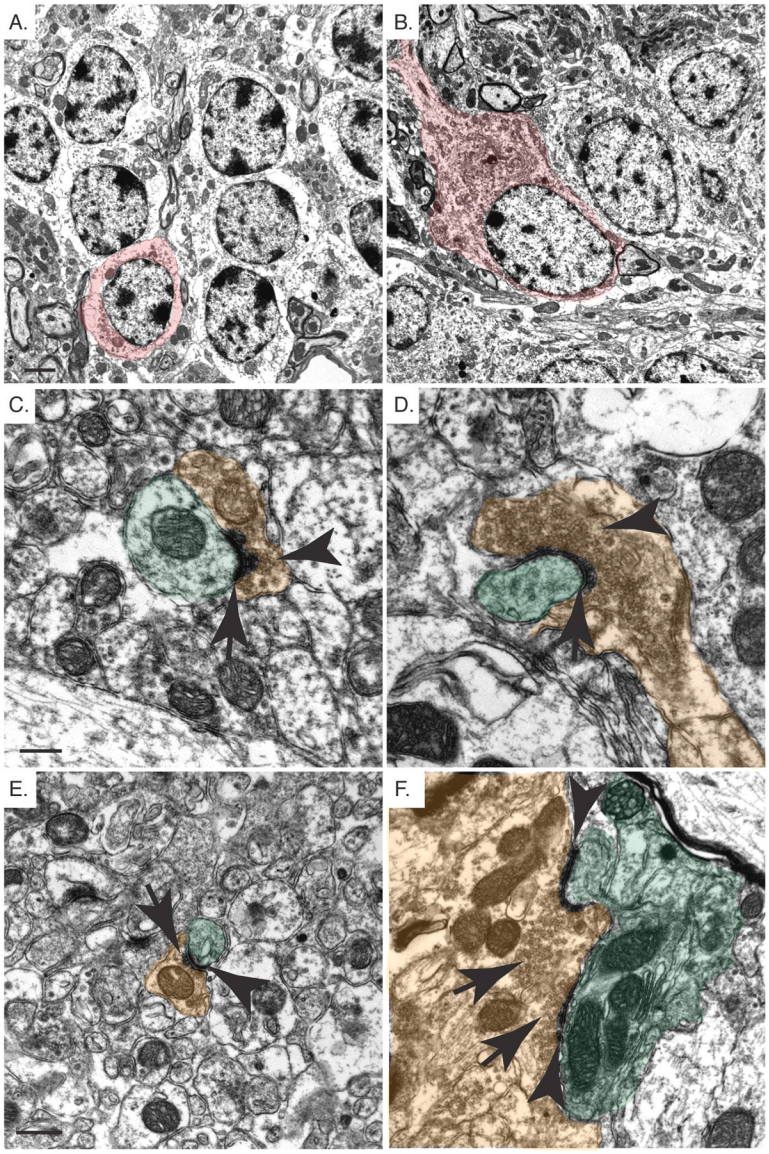

Fig. 4.

Structural abnormalities in Pten-deficient cerebellar granule neurons. A,B. Electron micrographs of the inner granule layer of control (A) and *Pten* cKO (B) mice. There is a significant enlargement of the granule neurons in the *Pten* cKO neurons compared with the control. The increased soma size is indicated with red color. These cells also have an increased ribosome density in the *Pten* cKO mice. C,D,E,F. Electron micrographs of the molecular layer from control (C,E) and *Pten* cKO (D,F) mice. Normal synapses containing a postsynaptic density (arrow) and pre-synaptic terminals containing synaptic vesicles (arrow head) are shown. The pre and post-synaptic terminals are indicated with brown and green color, respectively. The synapses in the *Pten* cKO (D,F) mice showed greatly enlarged pre-synaptic terminals with increased synaptic vesicles (arrow head) and postsynaptic densities (arrow) that engulfed the Purkinje cells. One pre-synaptic terminal is able to synapse with multiple post-synaptic terminals (F). Mice were >10 weeks old. Scale bar for A,B=2μm, C,D=0.3μm and E,F=0.5μm.

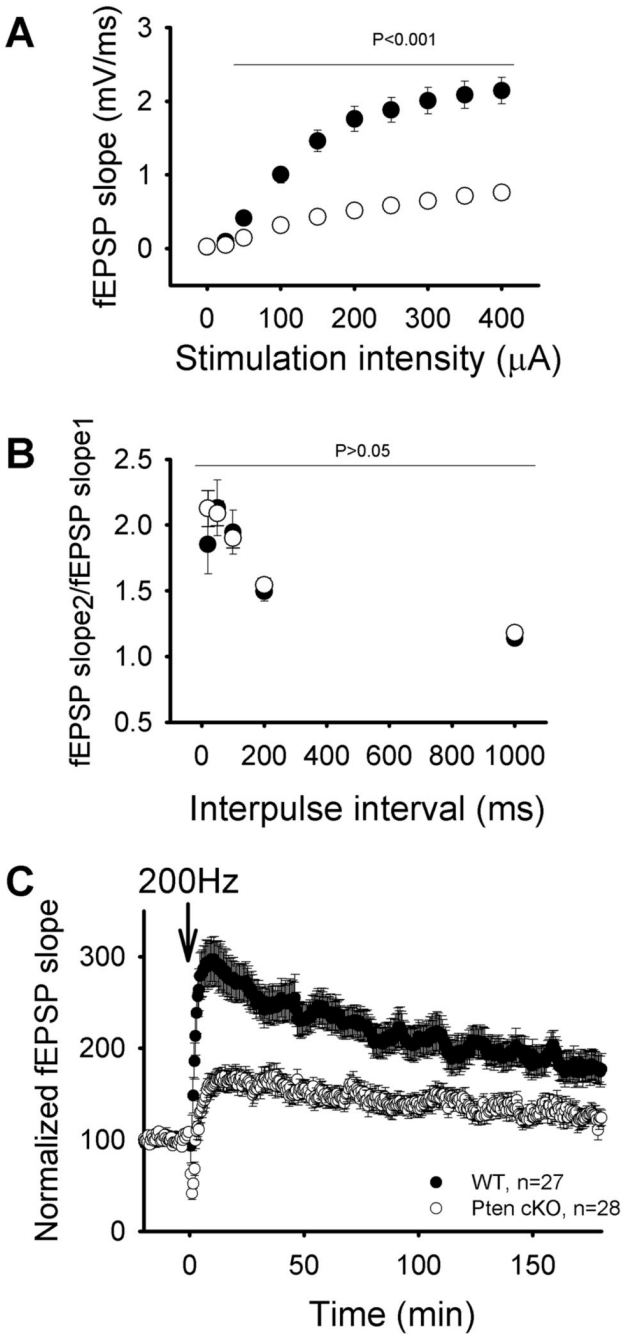

Fig. 5.

Synaptic transmission and synaptic plasticity are defective in *Pten* cKO mice. A. Mean fEPSPs as a function of stimulation intensity in *Pten* cKO mice and wild-type littermates. B. Pair-pulse ratio of two mean fEPSPs as a function of interstimulus interval measured in slices from *Pten* cKO and WT mice. C. Average fEPSPs *v*s time before and after 200 Hz tetanizations measured in Pten cKO and WT mice (downward arrows). Mice were 3.5 to 4 weeks of age.

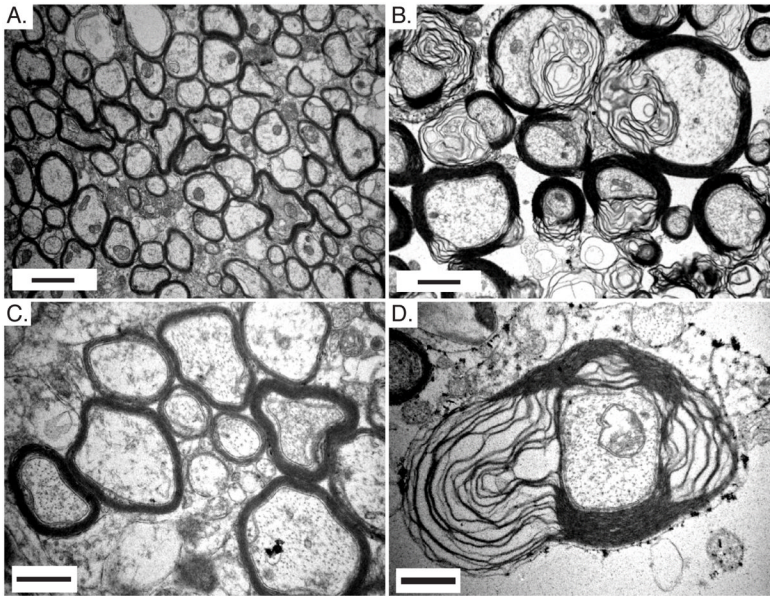

Fig. 6.

Abnormal myelination in *Pten* cKO mouse brains. A,B,C,D. Electron micrographs at two magnifications of the corpus callosum from adult control (A,C) and *Pten* cKO mice (B,D). Myelin thickness is increased and the myelin sheath is unraveling in *Pten* cKO mice compared with control mice. Mice were >10 weeks old. Scale bar for A,B=1μm and C,D=0.5μm.

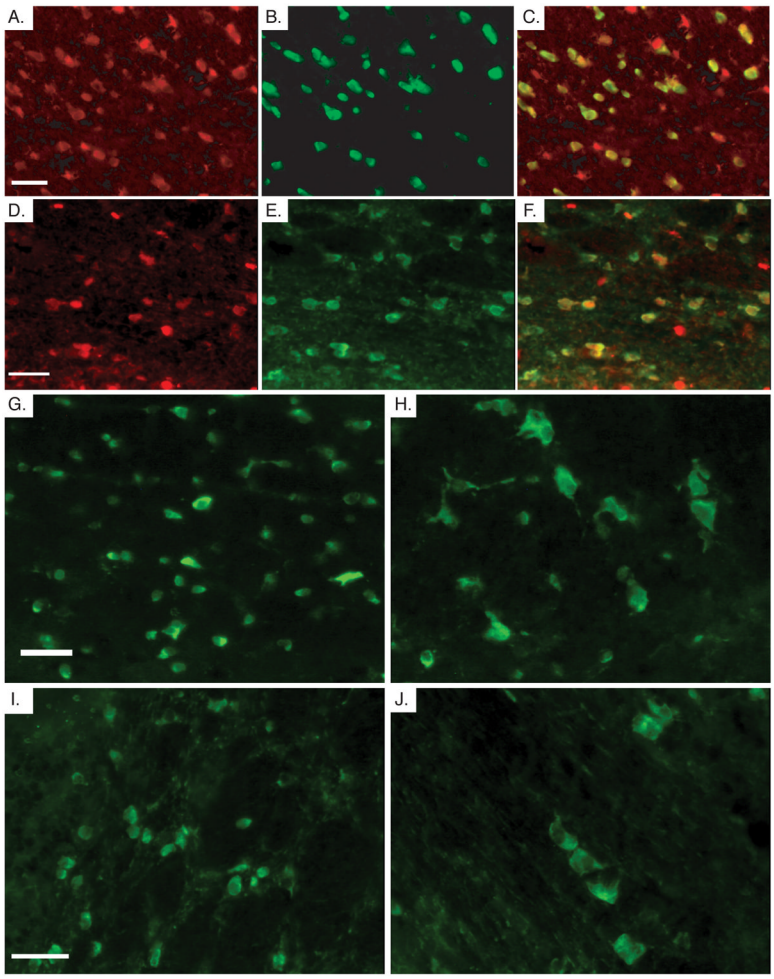

Fig. 7.

Cre activity in oligodendrocytes leads to hypertrophy. A,B,C. Immunofluorescence in the corpus callosum of adult *GFAP-cre;ROSA26R* mice shows β-Gal expression (A), CC-1 (B) and the overlay of the two images (C). D,E,F. Immunofluorescence in the white matter tracks of the cerebellum of adult *GFAP-cre;ROSA26R* brains showing β-Gal (D) and CC-1 (E), and the overlapping images (F). G,H. CC-1 immunofluorescence in the corpus callosum control (G) and *Pten* cKO mice (H). A population of CC-1 positive cells in the *Pten* cKO mice are significantly enlarged compared with the control CC-1 positive cells in the same region. I,J. CC-1 immunofluorescence in the white matter track of the cerebellum of control (I) and *Pten* cKO mice (J). Again, a population of oligodendrocytes are significantly enlarged in size in the *Pten* cKO mice. Mice were 4 weeks of age for A,B,C,D,E,F and mice were >10 weeks old for G,H,I,J. Scale bar for all=30μm.

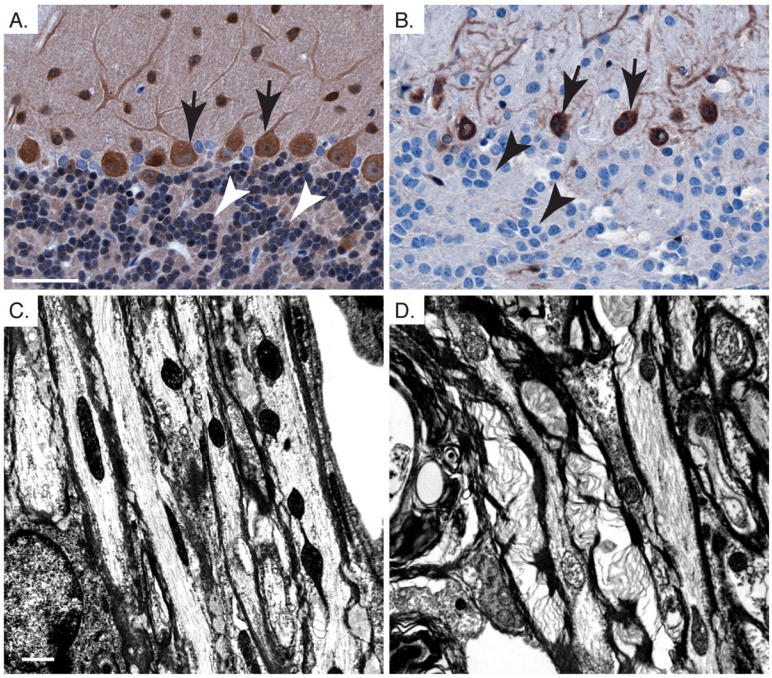

Fig. 8.

Pten loss in oligodendrocytes leads to cell autonomous defects in myelination in the cerebellum. A,B. Pten immunohistochemistry shows loss of Pten in granule neurons of the IGL (arrow head), and persistent Pten expression in Purkinje cells (arrows) from *Pten* cKO cerebellum (B) compared to control (A). C,D. Electron micrographs showing myelination in the cerebellar white matter tracks of control (A) and *Pten* cKO (B). Mice were >10 weeks old. Scale bar for A,B=50μm and C,D=1μm.